Available online at www.sciencedirect.com
SCIENCE DIRECT®
Physics Letters B 630 (2005) 31–39
PHYSICS LETTERS B
www.elsevier.com/locate/physletb

A measurement of the CP-conserving component of the decay $K_S^0 \to \pi^+\pi^-\pi^0$

J.R. Batley, C. Lazzeroni, D.J. Munday, M. Patel [1], M.W. Slater, S.A. Wotton

Cavendish Laboratory, University of Cambridge, Cambridge CB3 0HE, UK [2]

R. Arcidiacono, G. Bocquet, A. Ceccucci, D. Cundy [3], N. Doble, V. Falaleev, L. Gatignon, A. Gonidec, P. Grafström, W. Kubischta, F. Marchetto [4], I. Mikulec [5], A. Norton, B. Panzer-Steindel, P. Rubin [6], H. Wahl [7]

CERN, CH-1211 Genève 23, Switzerland

E. Goudzovski, D. Gurev, P. Hristov [1], V. Kekelidze, L. Litov, D. Madigozhin, N. Molokanova, Yu. Potrebenikov, S. Stoynev, A. Zinchenko

Joint Institute for Nuclear Research, Dubna, Russia

E. Monnier [8], E. Swallow, R. Winston

The Enrico Fermi Institute, The University of Chicago, Chicago, IL 60126, USA

R. Sacco [9], A. Walker

Department of Physics and Astronomy, University of Edinburgh JCMB King's Buildings, Mayfield Road, Edinburgh EH9 3JZ, UK

W. Baldini, P. Dalpiaz, P.L. Frabetti, A. Gianoli, M. Martini, F. Petrucci, M. Scarpa, M. Savrié

Dipartimento di Fisica dell'Università e Sezione dell'INFN di Ferrara, I-44100 Ferrara, Italy

A. Bizzeti [10], M. Calvetti, G. Collazuol [11], G. Graziani, E. Iacopini, M. Lenti, F. Martelli [12], G. Ruggiero [1], M. Veltri [12]

Dipartimento di Fisica dell'Università e Sezione dell'INFN di Firenze, I-50125 Firenze, Italy

0370-2693/$ – see front matter
doi:10.1016/j.physletb.2005.09.077

M. Behler, K. Eppard, M. Eppard [1], A. Hirstius [1], K. Kleinknecht, U. Koch, L. Masetti, P. Marouelli, U. Moosbrugger, C. Morales Morales, A. Peters [1], M. Wache, R. Wanke, A. Winhart

Institut für Physik, Universität Mainz, D-55099 Mainz, Germany [13]

A. Dabrowski, T. Fonseca Martin, M. Velasco

Department of Physics and Astronomy, Northwestern University, Evanston, IL 60208-3112, USA

G. Anzivino, P. Cenci, E. Imbergamo, G. Lamanna, P. Lubrano, A. Michetti, A. Nappi, M. Pepe, M.C. Petrucci, M. Piccini, M. Valdata

Dipartimento di Fisica dell'Università e Sezione dell'INFN di Perugia, I-06100 Perugia, Italy

C. Cerri, F. Costantini, R. Fantechi, L. Fiorini, S. Giudici, I. Mannelli, G. Pierazzini, M. Sozzi

Dipartimento di Fisica, Scuola Normale Superiore e Sezione dell'INFN di Pisa, I-56100 Pisa, Italy

C. Cheshkov [1], J.B. Cheze, M. De Beer, P. Debu, G. Gouge, G. Marel, E. Mazzucato, B. Peyaud, B. Vallage

DSM/DAPNIA, CEA Saclay, F-91191 Gif-sur-Yvette, France

M. Holder, A. Maier, M. Ziolkowski

Fachbereich Physik, Universität Siegen, D-57068 Siegen, Germany [14]

C. Biino, N. Cartiglia, M. Clemencic, S. Goy Lopez, E. Menichetti, N. Pastrone

Dipartimento di Fisica Sperimentale dell'Università e Sezione dell'INFN di Torino, I-10125 Torino, Italy

W. Wislicki

Soltan Institute for Nuclear Studies, Laboratory for High Energy Physics, PL-00-681 Warsaw, Poland [15]

H. Dibon, M. Jeitler *, M. Markytan, G. Neuhofer, L. Widhalm

Österreichische Akademie der Wissenschaften, Institut für Hochenergiephysik, A-1050 Wien, Austria [16]

Received 13 July 2005; accepted 26 September 2005

Available online 11 October 2005

Editor: W.-D. Schlatter

Abstract

The NA48 Collaboration has measured the amplitude of the CP-conserving component of the decay $K_S^0 \to \pi^+\pi^-\pi^0$ relative to $K_L^0 \to \pi^+\pi^-\pi^0$. For the characteristic parameter λ, the values $\mathrm{Re}\,\lambda = 0.038 \pm 0.010$ and $\mathrm{Im}\,\lambda = -0.013 \pm 0.007$ have been extracted. These values agree with earlier measurements and with theoretical predictions from chiral perturbation theory.

1. Introduction

The $K_S^0 \to \pi^+\pi^-\pi^0$ decay amplitude is dominated by two angular momentum components, $l = 0$ and $l = 1$ (l is the angular momentum of the neutral pion with respect to the system of the two charged pions); higher angular momentum states are suppressed because the kaon mass is close to the three pion mass. In this analysis we have measured the CP conserving transition to the $l = 1$ state through its interference with the dominant $K_L^0 \to \pi^+\pi^-\pi^0$ decay. We neglect any effects from CP violation in mixing and decay, which are totally negligible at our level of sensitivity.

The amplitudes for the decays of neutral kaons into three pions ($A_L^{3\pi}$ for K_L^0 and $A_S^{3\pi}$ for K_S^0) can be parameterized in terms of the Dalitz variables X and Y, which are defined as

$$X = \frac{s_{\pi^-} - s_{\pi^+}}{m_{\pi^\pm}^2}, \qquad Y = \frac{s_{\pi^0} - s_0}{m_{\pi^\pm}^2} \tag{1}$$

with $s_\pi = (p_K - p_\pi)^2$, $s_0 = \frac{1}{3}(s_{\pi^+} + s_{\pi^-} + s_{\pi^0})$ and p_K and p_π being the 4-momenta of the kaon and the pion, respectively. The Dalitz variable X is a measure of the difference of the energies of the two charged pions in the kaon's rest system while Y is a measure of the energy of the neutral pion in the kaon's rest system.

The $l = 1$ and the $l = 0$ components of the decay $K_S^0 \to \pi^+\pi^-\pi^0$ can be separated by the fact that the amplitude of the $l = 1$ process is antisymmetric in X while the $l = 0$ process is symmetric in X. Therefore the $l = 1$ contribution can be extracted by separately integrating over the regions $X > 0$ and $X < 0$ and subtracting the results from each other. We consider the distribution

$$V(t) = \frac{N_{3\pi}^{X>0}(t) - N_{3\pi}^{X<0}(t)}{N_{3\pi}^{X>0}(t) + N_{3\pi}^{X<0}(t)}, \tag{2}$$

where $N_{3\pi}^{X>0}(t)$ [$N_{3\pi}^{X<0}(t)$] is the number of decays of neutral kaons into $\pi^+\pi^-\pi^0$ at time t with a value of the Dalitz variable X larger [smaller] than zero [1,2].

In the NA48 set-up, where K_S^0 and K_L^0 are produced in equal amounts at a fixed target, the interference of the $l = 1$ component of $K_S^0 \to \pi^+\pi^-\pi^0$ with the $l = 0$ component of the dominant $K_L^0 \to \pi^+\pi^-\pi^0$ decay can be observed. It can be described by a complex pa-

* Corresponding author.
E-mail address: manfred.jeitler@cern.ch (M. Jeitler).
[1] Present address: CERN, CH-1211 Genève 23, Switzerland.
[2] Funded by the UK Particle Physics and Astronomy Research Council.
[3] Present address: Istituto di Cosmogeofisica del CNR di Torino, I-10133 Torino, Italy.
[4] On leave from Sezione dell'INFN di Torino, I-10125 Torino, Italy.
[5] On leave from Österreichische Akademie der Wissenschaften, Institut für Hochenergiephysik, A-1050 Wien, Austria.
[6] On leave from University of Richmond, Richmond, VA 23173, USA; supported in part by the US NSF under award #0140230.
[7] Also at Dipartimento di Fisica dell'Università e Sezione dell'INFN di Ferrara, I-44100 Ferrara, Italy.
[8] Also at Centre de Physique des Particules de Marseille, IN2P3-CNRS, Université de la Méditerrané, Marseille, France.
[9] Present address: Department of Physics, Queen Mary College, University of London, Mile End Road, London E1 4NS, UK.
[10] Dipartimento di Fisica dell'Università di Modena e Reggio Emilia, via G. Campi 213/A I-41100, Modena, Italy.
[11] Present address: Scuola Normale Superiore e Sezione dell'INFN di Pisa, I-56100 Pisa, Italy.
[12] Istituto di Fisica, Università di Urbino, I-61029 Urbino, Italy.
[13] Funded by the German Federal Minister for Research and Technology (BMBF) under contract 7MZ18P(4)-TP2.
[14] Funded by the German Federal Minister for Research and Technology (BMBF) under contract 056SI74.
[15] Supported by the Committee for Scientific Research grants 5P03B10120, SPUB-M/CERN/P03/DZ210/2000 and SPB/CERN/P03/DZ146/2002.
[16] Funded by the Austrian Ministry for Traffic and Research under contract GZ 616.360/2-IV GZ 616.363/2-VIII, and by the Fonds für Wissenschaft und Forschung FWF No. P08929-PHY.

rameter [3]

$$\lambda = \frac{\int_{-\infty}^{\infty} dY \int_{0}^{\infty} dX\, A_L^{*3\pi(l=0)}(X,Y) A_S^{3\pi(l=1)}(X,Y)}{\int_{-\infty}^{\infty} dY \int_{0}^{\infty} dX\, |A_L^{3\pi(l=0)}(X,Y)|^2}, \tag{3}$$

which has been extracted by fitting the distribution defined above:

$$V(t) \approx 2D(E)\big[\mathrm{Re}(\lambda)\cos(\Delta m t) - \mathrm{Im}(\lambda)\sin(\Delta m t)\big] \times \frac{e^{-\frac{t}{2}(\frac{1}{\tau_S}+\frac{1}{\tau_L})}}{e^{-\frac{t}{\tau_L}}}. \tag{4}$$

Δm is the mass difference between K_L^0 and K_S^0, τ_L and τ_S are the respective lifetimes, and the energy-dependent "dilution" $D(E)$ is the difference in the relative abundances of K^0 and $\bar{K}^0$ at production for a kaon energy of E:

$$D(E) = \frac{K^0 - \bar{K}^0}{K^0 + \bar{K}^0}. \tag{5}$$

2. Experimental setup

The data presented here were taken in a high-intensity neutral beam at the CERN Super Proton Synchrotron during 89 days in 2002. Protons of 400 GeV with an average intensity of 5×10^{10} per 4.8 s spill (within a cycle of 16.2 s) impinged on a beryllium target, where secondary particles were produced. Charged particles were removed by a sweeping magnet and a 5.1 m long collimator, which selected a beam of neutral particles at an angle of 4.2 mrad with respect to the proton beam.

After the collimator, the neutral beam and the decay products propagated in an 89 m long vacuum tank, where most of the short-lived kaons (K_S^0) and neutral hyperons (Λ^0, Ξ^0), as well as a small fraction of the long-lived neutral kaons (K_L^0) decayed. Undecayed particles (K_L^0, neutrons) continued to a beam dump via a vacuum pipe that passed through all of the downstream detectors.

Downstream of the vacuum tank there was a magnetic spectrometer consisting of four drift chambers inside a helium-filled tank and a magnet with a horizontal transverse momentum kick of 265 MeV/c. The spatial resolution was 120 μm per view, and the momentum resolution was $\delta p/p = (0.48 \oplus 0.015p)\%$, with momentum p in GeV/c.

After the spectrometer there was a scintillator hodoscope, for the accurate timing of charged particles (yielding a time resolution on single tracks of 250 ps), and a liquid-krypton electromagnetic calorimeter, for the measurement of photons and electrons, with an energy resolution of $\sigma(E)/E = (3.2/\sqrt{E} \oplus 9/E \oplus 0.42)\%$ (E in GeV). These were followed by a hadron calorimeter and a muon detector. A more detailed description of the detector has been given elsewhere [4].

3. The trigger

Decays into $\pi^+\pi^-\pi^0$ made up only a small part of the event rate in the detector. This was due to the small expected branching ratio for the K_S^0 decay and to the long lifetime of the K_L^0. To obtain a statistically significant sample of $\pi^+\pi^-\pi^0$ decays, a very selective trigger was used to suppress the high two-particle background, which came mostly from $K_S^0 \to \pi\pi$ and from $\Lambda^0 \to p\pi^-$.

When the level-1 trigger indicated an event with at least two charged tracks and a minimum energy deposition of 30 GeV in the calorimeters, a fast online processor calculated the momenta of the charged tracks, and hence the invariant mass of the decaying neutral particle under the assumptions of $K_S^0 \to \pi^+\pi^-$, $\Lambda^0 \to p\pi^-$, and $\bar{\Lambda}^0 \to \bar{p}\pi^+$. Events were accepted by the trigger if none of the calculated masses matched the physical mass of the particle in question (difference of squares of the calculated mass and the nominal mass [5] larger than two percent). Additional cuts were applied to the relative momenta of the two charged particles ($p_{\mathrm{larger}}/p_{\mathrm{smaller}} < 3.5$, to further suppress Λ^0 decays) and to the separation of the two tracks at the entry of the spectrometer (> 5 cm in drift chamber 1, to remove photon conversions in the upstream Kevlar window). To allow a measurement of the trigger efficiency, a downscaled sample of minimum-bias events (1/35) was recorded in parallel, where only the level-1 trigger condition was fulfilled. In the course of data-taking, the high voltage in the drift chambers was occasionally adjusted to maintain stable operating conditions. As a result, the efficiency of the level-2 trigger varied between $(75 \pm 4)\%$ and

$(86 \pm 4)\%$. By comparing the analysis of different time periods, it was checked that this variation did not introduce any spurious asymmetries.

4. Data analysis

For the offline analysis, events were selected with two tracks of opposite charge from the same vertex (distance of closest approach less than 3 cm), and at least two electromagnetic clusters (within ± 20 ns). For each pair of clusters, the π^0-mass was calculated assuming that the pion decayed at the position of the charged vertex. If there were more than two clusters, the cluster pair yielding the best π^0-mass was retained.

In order to reduce acceptance effects near the edges of the detectors, each charged track was required to cross the drift chambers at a minimum distance of 12 cm and a maximum distance of 110 cm from the beam axis. Likewise, each photon cluster was required to be more than 15 cm from the beam axis and more than 10 cm from the outer edge of the calorimeter.

In addition, the photon clusters had to be well separated from tracks (> 15 cm) to avoid mismeasurements due to energy sharing. Tracks were identified as charged pions rather than electrons by demanding that their electromagnetic energy deposition was less than 90 percent of the track momentum. Cuts were applied on the charged vertex (less than 3 cm lateral distance from the K^0 beam line, and between 800 and 5400 cm from the target), and on the masses reconstructed for $K^0 \to \pi^+\pi^-\pi^0$ and $\pi^0 \to \gamma\gamma$ ($m_{K^0}^{\mathrm{PDG}} \pm 10.5$ MeV and $m_{\pi^0}^{\mathrm{PDG}} \pm 7.8$ MeV [5]). These cuts also excluded $K_S^0 \to \pi^+\pi^-$ decays. The reconstructed kaon energy was required to be between 30 and 166 GeV. Λ^0 hyperons were further suppressed by cutting harder than in the trigger on the masses for the hypotheses $\Lambda^0 \to p\pi^-$ and $\bar{\Lambda}^0 \to \bar{p}\pi^+$ ($m_{\Lambda^0}^{\mathrm{PDG}} \pm 21$ MeV [5]) and on the momentum ratio of the two charged particles ($p_{\mathrm{larger}}/p_{\mathrm{smaller}} < 2.9$). No Λ^0 hyperons survive after these two cuts. The mass cuts were optimized to maintain a high efficiency without introducing substantial background. A total of 19 million events passed all these cuts.

Fig. 1 shows the distributions of the position of decay vertices along the beam line (z vertex) and the reconstructed K^0 energy after applying the analysis cuts.

Fig. 2 shows the distribution of the K^0 invariant mass after cuts.

Applying these cuts and correcting for acceptance and trigger efficiency as described below, the experimental distribution $V(t)$ defined in (2) was obtained. The values of $\mathrm{Re}\,\lambda$ and $\mathrm{Im}\,\lambda$ were extracted by fitting equation (4) to the experimental data. Due to the energy dependence of the dilution $D(E)$, the fit was made in bins of kaon energy (see Fig. 3), with 8 equal-sized energy bins ranging from 30 to 166 GeV. The

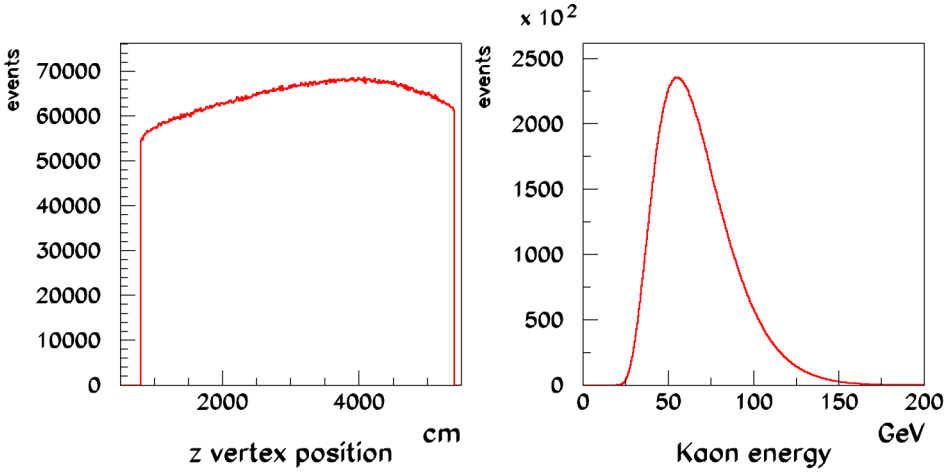

Fig. 1. Position of the decay vertex along the beam line (left, measured from target position) and reconstructed K^0 energy (right) for the data sample of 19 million events.

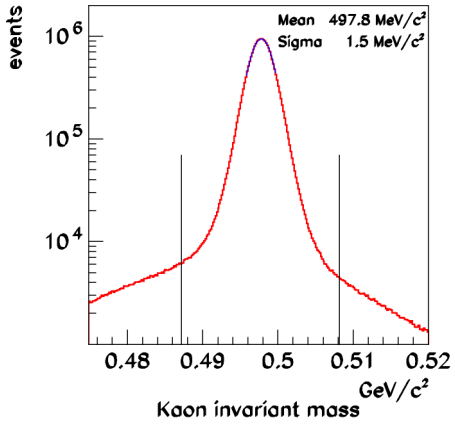

Fig. 2. The K^0 invariant mass. The vertical lines indicate the K^0 mass cut used in the analysis.

values for the external parameters Δm, τ_L and τ_S were taken from [5]. For the dilution $D(E)$, we used a quadratic fit to the values measured in [6] (energy E given in GeV)

$$D_{\text{measured}}(E) = -0.167 + \frac{6.10}{10^3}E - \frac{1.72}{10^5}E^2. \qquad (6)$$

The errors for the individual points measured in [6] vary between 5 percent at the lowest kaon energies (75 GeV) and 25 percent at the highest energies (165 GeV). We assume the uncertainties at the different energies to be uncorrelated. To take into account the difference in proton energy and production angle between [6] and our own measurement, we used measurements with charged kaons [7], from which we derived an empirical correction factor (energy E given in GeV)

$$D_{\text{corr}}(E) = 1.28 - \frac{3.82}{10^3}E + \frac{5.38}{10^5}E^2 - \frac{3.32}{10^7}E^3 + \frac{7.15}{10^{10}}E^4. \qquad (7)$$

To fit Eq. (4), we then use

$$D(E) = D_{\text{measured}}(E) \times D_{\text{corr}}(E). \qquad (8)$$

Based on the uncertainties in [6,7], the overall relative uncertainty in $D(E)$ is estimated at about 15 percent.

The aim of the experiment was to measure a small effect that is antisymmetric in the Dalitz variable X (the interference of K_S^0 and K_L^0 in the decay into $\pi^+\pi^-\pi^0$) over a large background that is symmetric in X (from the CP-conserving decay $K_L^0 \to \pi^+\pi^-\pi^0$). Therefore, care had to be taken to exclude any detector effects that could artificially introduce such an asymmetry in the K_L^0 decay.

The sign of X equals the sign of the momentum difference of the π^+ and the π^- in the kaon rest system. The pion momenta in the kaon rest system are correlated to their momenta in the laboratory system. Any momentum-dependent difference in the acceptance or the trigger efficiency for positive and negative pions may therefore introduce a possible bias. Due to the field of the spectrometer magnet, positive and negative particles populated the detector in a different way. In order to compensate such effects, the field of the spectrometer magnet was reversed weekly during the data taking.

An artificial asymmetry can be caused by the detector acceptance only if this acceptance is asymmetric in X. However, if there is a real, physical asymmetry, its value may be distorted even by a symmetric X-dependence of the acceptance. The NA48 detector simulation (based on the GEANT3 package [8]) showed a symmetric decrease in the acceptance for high $|X|$. Using the simulation, the acceptance was calculated as a function of $|X|$, kaon decay time and kaon energy. The effect was then corrected by weighting each event in the data in inverse proportion to the calculated acceptance for the corresponding value of $|X|$, kaon decay time and kaon energy. This procedure resulted an increase of 10 ± 5 percent in the extracted values of $\text{Re}\,\lambda$ and $\text{Im}\,\lambda$.

In the drift chambers, signal attenuation near the ends of some wires created a left–right acceptance asymmetry on the detector periphery, especially for strongly deviated low-momentum particles. This was compensated in the offline reconstruction by the redundancy of chamber planes, and there was no visible effect on the minimum-bias data sample. However the data collected with the fast level-2 trigger algorithm, which did not use the full redundancy, showed an asymmetry in X at all kaon lifetimes, which was strongest (2 percent) at the lowest kaon energies (30 GeV). This asymmetry was reversed when the magnetic field of the spectrometer magnet was inverted. Using the X-symmetric amplitude of $K_L \to \pi^+\pi^-\pi^0$, the detector and trigger simulation accurately reproduced this behavior.

The Monte Carlo distributions from the simulation were used to correct the data. The correction resulted

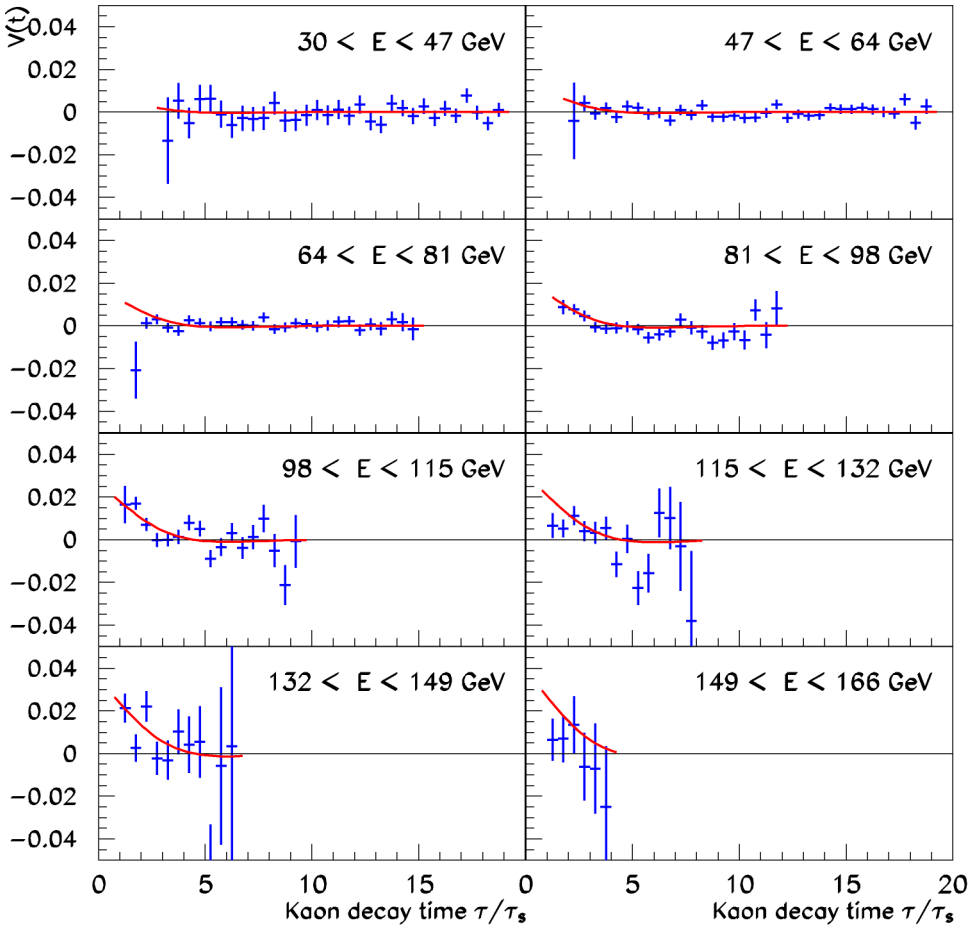

Fig. 3. The experimental distribution $V(t)$ (points with error bars) and the function obtained by a χ^2 fit (smooth curve) in bins of time and energy. The χ^2 per degree of freedom is $169.35/162 = 1.045$. The fit was made simultaneously over all energy bins, but is mainly constrained by the intermediate energy bins. The data were compensated for acceptance and trigger efficiency by applying Monte Carlo corrections and by averaging over samples with opposite magnetic field in the spectrometer.

in a shift of about 3×10^{-2} in both $\mathrm{Re}\,\lambda$ and $\mathrm{Im}\,\lambda$, with opposite sign for the two field orientations of the spectrometer magnet. The simulation program had been developed, extensively used and validated during previous studies by the collaboration [4,9]. After acceptance and trigger corrections, the individual results for the two field orientations differ by about 1.4σ. To exclude possible additional effects the Monte Carlo corrected data samples with positive and negative fields in the spectrometer were subsequently averaged (taking the arithmetic mean of the observed distributions $V(t)$ in formula (2), which is equivalent to normalizing the data taken in the two field orientations to the same number of events and summing them before applying (2)). Slightly different results were obtained when using either only the Monte Carlo correction (without averaging over the two magnetic field orientations), or only averaging over the magnetic fields (without the Monte Carlo correction). We use half the difference between these two last approaches as a contribution to our systematic error (± 0.004 in $\mathrm{Re}\,\lambda$ and ± 0.003 in $\mathrm{Im}\,\lambda$).

Another cross-check was to analyse the data with a tight outer radius cut of 50 cm in the drift chambers and otherwise follow the above procedure. This was prompted by the fact that the observed drift chamber inefficiencies were highest at large radii. The results in $\mathrm{Re}\,\lambda$ and $\mathrm{Im}\,\lambda$ differed by about 0.001 while

the statistical errors increased by about the same amount.

The other major contribution to the systematic uncertainty comes from the $K^0/\bar{K}^0$ dilution $D(E)$ defined in formula (5) and leads to an additional uncertainty of ± 0.005 in $\mathrm{Re}\,\lambda$ and of ± 0.003 in $\mathrm{Im}\,\lambda$. By varying the experimental cuts quoted above within reasonable bounds and the external parameters from [5] within their errors it was seen that all other possible sources of systematic uncertainties were negligible.

5. Results

The following values have been obtained for the real and imaginary parts of λ:

$$\mathrm{Re}\,\lambda = +0.038 \pm 0.008_{\mathrm{stat}} \pm 0.006_{\mathrm{syst}}, \tag{9}$$

$$\mathrm{Im}\,\lambda = -0.013 \pm 0.005_{\mathrm{stat}} \pm 0.004_{\mathrm{syst}}. \tag{10}$$

Adding both errors in quadrature,

$$\mathrm{Re}\,\lambda = +0.038 \pm 0.010, \tag{11}$$

$$\mathrm{Im}\,\lambda = -0.013 \pm 0.007. \tag{12}$$

These values can be compared with the theoretical numbers of $\mathrm{Re}\,\lambda = +0.031$ and $\mathrm{Im}\,\lambda = -0.006$ obtained in [3] by using results from chiral perturbation theory [2].

Fig. 4 shows the distribution $V(t)$ defined in (2) derived from the data, and the curve obtained from (4) with the fitted values of $\mathrm{Re}\,\lambda$ and $\mathrm{Im}\,\lambda$. These values were not obtained by fitting this histogram directly, but by fitting all data in bins of energy. This is important because of the dependence of the dilution $D(E)$ on the kaon energy.

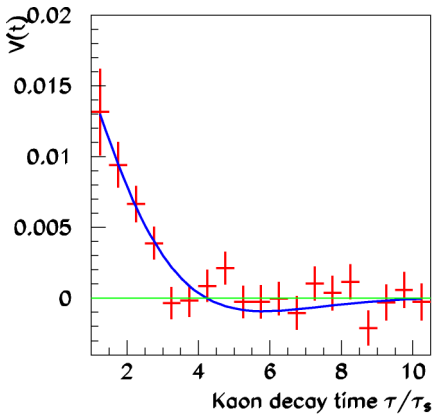

Fig. 4. The experimental distribution $V(t)$ (points with error bars, data summed over all kaon energies) and the function obtained from the fitted values for $\mathrm{Re}\,\lambda$ and $\mathrm{Im}\,\lambda$ for a mean kaon energy of 87 GeV.

The real and imaginary parts of λ are strongly correlated, as can be seen from Fig. 5, which shows the measured values and contours of equal χ^2 in the complex plane. Taking into account only the statistical errors, the correlation coefficient between $\mathrm{Re}\,\lambda$ and $\mathrm{Im}\,\lambda$ is 0.66.

From the real part of λ, the branching ratio for the CP-conserving component of the decay $K_S^0 \to \pi^+\pi^-\pi^0$ can be obtained. Using the same approximation and the external parameters as in [3], we get

$$\mathrm{BR}\left(K_S^0 \to \pi^+\pi^-\pi^0\right) = \left(4.7\ {}^{+2.2}_{-1.7}(\mathrm{stat})\ {}^{+1.7}_{-1.5}(\mathrm{syst})\right) \times 10^{-7}.$$

The results from this experiment agree with chiral perturbation theory and with two other measurements with comparable errors [3,10]. It is worth noting that experiment [3] used tagged kaons, so that its result is independent of any measurements or calculations of the dilution $D(E)$ while [10] was carried out at higher kaon energies and therefore higher dilution than our measurement. It should also be noted that all three experiments obtain a nonzero negative value for the imaginary part of λ (which is predicted to be small).

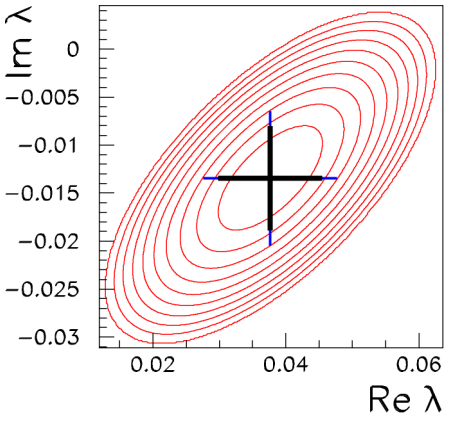

Fig. 5. The fitted values of $\mathrm{Re}\,\lambda$ and $\mathrm{Im}\,\lambda$ in the complex plane with the contours for a χ^2 of 1 to 10 above the minimum χ^2. The shorter error bars and the contours refer only to the statistical uncertainty while the longer error bars correspond to the total uncertainty.

Acknowledgements

It is a pleasure to thank the technical staff of the participating laboratories, universities and affiliated computing centers for their efforts in the construction of the NA48 apparatus, in the operation of the experiment, and in the processing of the data. We would also like to thank Maria Fidecaro for useful discussions.

References

[1] G. D'Ambrosio, N. Paver, Phys. Rev. D 49 (1994) 4560.
[2] G. D'Ambrosio, et al., Phys. Rev. D 50 (1994) 5767.
[3] A. Angelopoulos, et al., Eur. Phys. J. C 5 (1998) 389.
[4] A. Lai, et al., Eur. Phys. J. C 22 (2001) 231;
J.R. Batley, et al., Phys. Lett. B 576 (2003) 43.
[5] Particle Data Group, Review of Particle Physics, Phys. Lett. B 592 (2004).
[6] R. Carosi, et al., Phys. Lett. B 237 (1990) 303.
[7] H.W. Atherton, et al., CERN report 80-07, Geneva, 1980.
[8] GEANT Detector Description and Simulation Tool, CERN Program Library Long Write-up W5013, 1994.
[9] J.R. Batley, et al., Phys. Lett. B 544 (2002) 97.
[10] Y. Zou, et al., Phys. Lett. B 369 (1996) 362.